

How Many Hops Can Self-Backhauled Millimeter Wave Cellular Networks Support?

Mandar N. Kulkarni, Amitava Ghosh, and Jeffrey G. Andrews

Abstract—This paper considers the following question for viable wide-area millimeter wave cellular networks. What is the maximum extended coverage area of a single fiber site using multi-hop relaying, while achieving a minimum target per user data rate? We formulate an optimization problem to maximize the minimum end-to-end per user data rate, and exploit unique features of millimeter wave deployments to yield a tractable solution. The mesh network is modeled as a k -ring urban-canyon type deployment, where k is the number of hops back to the fiber site. Thus, the total number of relays per fiber site grows as k^2 . We consider both integrated access-backhaul (IAB) and orthogonal access-backhaul (OAB) resource allocation strategies, as well as both half and full duplex base stations (BSs). With a few validated simplifications, our results are given as simple closed-form expressions that are easy to evaluate even for large networks. Several design guidelines are provided, including on the choice of routing and scheduling strategy, the maximum allowable self-interference in full duplex relays and role of dual connectivity to reduce load imbalance across BSs. For example, we show that usually there is very little gain to IAB (as considered for 5G) as opposed to OAB (using separate spectrum for access and backhaul links); the latter being significantly simpler to implement.

I. INTRODUCTION

In order to deploy affordable millimeter wave (mmWave) cellular networks that can cover a large urban area, it is highly desirable to deploy self-backhauled networks [1]–[3], wherein a fraction of the base stations (BSs) have fiber-like backhaul and the rest of the BSs backhaul to the fiber sites wirelessly. This introduces a tradeoff between deployment cost and end user rate, which decreases as the amount of multi-hop relaying increases. Although such a mesh network architecture has been considered both theoretically and in practice many times in the past (as discussed next), with limited success, a few novel features of urban mmWave cellular systems lends to significant simplification. In particular, the highly directional transmissions, strong blocking from buildings, and limited diffraction around corners [4]–[7] – combined with an urban topography – allow us to plausibly model the network as a noise-limited k -ring deployment model, as shown in Fig. 1, with BSs deployed on a 2-D square grid. The number of relays grows as k^2 with a fixed inter-site distance (ISD). We consider a single fiber site, ignoring edge effects, which maybe anyway negligible due to the noise-limitedness. This model will allow us to succinctly quantify the maximum rate achievable by all users, called max-min rates, in closed form.

Email: mandar.kulkarni@utexas.edu, jandrews@ece.utexas.edu, amitava.ghosh@nokia-bell-labs.com. M. Kulkarni and J. Andrews are with the University of Texas at Austin, TX. A. Ghosh is with Nokia Bell Labs, Naperville, IL. Last revised on July 18, 2022.

We focus on max-min rates for two reasons. The first is that it allows us to determine the maximum value of k , that is how far the mesh network can extend from the fiber site, while ensuring a certain end-to-end (e2e) per user data rate. The second is that it results in a tractable optimization problem, as opposed to focusing on say, the 5th percentile user. We provide several validations of the proposed model and results. Given these tractable results, we consider three additional design choices, namely (i) integrated access-backhaul (IAB) or orthogonal access-backhaul (OAB) resource allocation, (ii) full or half duplex relays, and (iii) does dual connectivity improve per user rates in a self-backhauled network? IAB allows access and backhaul links to share time-frequency resources, whereas OAB reserves different set of resources for access and backhaul links.

A. Background, Motivation, and Related Work

The study of multi-hop wireless networks has a rich history spanning theoretically optimal resource allocation schemes [8]–[11], scaling laws [12], [13] and analysis of achievable e2e metrics [14]–[16]. There has also been industry-driven standardization activities for multi-hop wireless local area networks (WLANs) [17] and for fourth generation (4G) cellular networks with a single wireless backhaul hop [18], [19]. Practical implementation of multi-hop networks, however, has not been very successful. Reasons include the coupled interference and scheduling between hops [16], large overheads for maintaining multi-hop routes, a lack of Shannon-like theoretical limits and their corresponding design guidance [20] and the fundamentally poor e2e-rate scaling caused by each packet having to be transmitted multiple times [12].

A key differentiating factor for mmWave cellular networks is that they can be designed to be noise-limited, especially with large bandwidths and small antenna beam widths [3], [21]. This noise-limitedness greatly simplifies the routing and multi-hop scheduling problems and can help to close the gap between theoretically optimal solutions and practical implementations. For example, recently [22] proposes a polynomial time algorithm for joint routing and scheduling, extending the work in [8], unlike traditional NP-hard solutions [9], [11]. However, [22] considers a generic deployment topology and exploiting specific deployment patterns may result in even simpler structural solutions for optimal routing and scheduling. For example, in this paper we prove (for specific load scenarios) the optimality of a static routing scheme for urban canyon deployments, called *nearest neighbour highway routing*. Additionally, we observe it to be optimum more

generally using empirical studies. Another reason in favor multi-hop mmWave cellular networks is that many high data rate 5G applications have limited or no mobility, such as fixed wireless-to-home, industrial automation, or pedestrian/static mobile broadband users [2]. For future mobile applications, multi-connectivity, where users connect to multiple BSs at a time potentially operating over different frequency bands, may be exploited to offer smooth handovers in mmWave networks [23].

This new-found interest in multi-hopping for mmWave is reflected in recent academic work such as [3], [22], [24]–[30], as well as in 3GPP-Release 16 standardization activities [31]. A cross layer optimization framework was proposed in [24]. In [26], a fixed demand per flow traffic model was assumed to solve the problem of minimizing the time to empty the demands of all flows. In [25], a joint cost minimization along with resource allocation optimization problem was formulated. In [3], [30], per user rate analysis in mmWave self-backhauled networks was done using stochastic geometry considering a single backhaul hop. These frameworks do not trivially extend to analysis of multi-hop backhauling. Note that in most of the prior works which attempted to optimize resources in multi-hop mmWave networks the optimal solutions are NP-hard or require implementing a linear program that involve large matrices with the size growing very fast with the number of nodes in the network [22], [27], although approximate simpler solutions have been attempted [22], [26], [29]. The closest recent work to this work is [28], which considers a general graph for deployment and includes out of cell interference leading to a linear programming solution for joint routing and scheduling. This is where our work differs, as we use noise-limitedness to exactly solve the optimization problem under consideration to give closed form results for maximizing minimum rate in the network considering different design choices and also provide structural results on optimal routing. We later show the utility of these results by comparing with empirical studies incorporating interference.

B. Contributions

Closed form results for max-min optimal rates. We propose to study a grid deployment of BSs with a single fiber site and k^2 relays around it, which we term a k -ring deployment. Arbitrary but static user equipment (UE) deployment is assumed with full buffer traffic. UEs can be uplink (UL) or downlink (DL). We compute closed form expressions of maximum e2e rate achievable by all UEs when the BSs are half or full duplex, and when IAB or OAB resource allocation strategy is used. All rates are assumed to be deterministic, although our results for OAB hold can be extended when access rates are random. We first compute the max-min rates with simplifying assumptions on load across different BSs, and assume equal access rates for all users to come up with a simple formula. Optimality of nearest neighbor highway routing, defined in Section III, is shown in this scenario but is later observed to hold in greater generality. The analytical result is then extended considering a more general setup of unequal access rates to different users, and arbitrary load per BS.

Applications of the analysis. We answer the titular question under several realistic network parameters for BSs spaced at $D = 200$ m and operating at 28 GHz carrier frequency with 800 MHz bandwidth. If 1024 QAM is the maximum size of constellation supported, up to 4 ring deployments can offer 100 Mbps per UE considering a load of 2 NLOS UEs per BS separated at 100m from the serving BSs. If even higher order modulations are used, up to 6 ring deployments can be supported with 2 UEs per BS for practical values of antenna gains and $D = 100$ m. The max-min rates derived are also used to compare IAB versus OAB, single versus dual connectivity and half versus full duplex base stations, which also lead to interesting insights detailed in Section V. For instance, it is possible to closely follow the max-min rates with IAB using an OAB scheme which can be simpler to implement in practice.

Positive side-effects of network bottlenecks. We observe that our noise-limited analysis is accurate not just because of large bandwidth or narrow beam widths, but also for the following reason. The proposed deployment has very few bottleneck links in many load scenarios considering reasonably large antenna gains (greater than 16 UE antennas and 64 BS antennas [32]) such that most NLOS UE access links are not bottlenecks. Thus, the optimal scheduler can meet the theoretically optimal max-min rates by just activating few links at a time, leading to noise-limited system performance. Another positive side-effect of network bottlenecks is that the analysis can be used as a benchmarking tool for complex simulators which emulate proportional fairness (PF) in multi-hop networks. We show an illustrative example which also highlights that k -ring deployments can be noise-limitedness even if the schedulers are not interference aware owing to blockage effects and directionality of mmWave networks.

II. SYSTEM MODEL

k -ring deployment. We propose to study a k -ring deployment model for urban canyon scenarios, as shown in Fig. 1. Lines represent streets on which BSs are deployed, with BSs denoted by either a triangle (MBS) or star (relays). The inter-line spacing is D meters. The MBS, which is the fiber backhauled BS or master BS, is located at $(0, 0)$ and the relays are located at (iD, jD) for $i, j \in \{0, \pm 1, \pm 2, \dots, \pm k\}$ such that the Manhattan distance from any relay to the MBS is $\leq kD$. We denote (iD, jD) by (i, j) . BSs separated by a distance D are LOS. Fig. 2 shows a heuristic k -ring deployment ($k = 4$, $D = 100$ m) in Chicago’s downtown, which indicates it is a reasonable model. All possible links (directed line joining any two nodes, which can be BSs or UEs) in the network are wireless.

Performance is evaluated for a static realization of UE locations, motivated from fixed wireless to home or other low mobility applications. The analysis in Section III works for arbitrary UE locations, and specific assumptions on access rates to different UEs will be made later while discussing the results. Let U be the total number of UEs. Each UE associates with one BS according to a any association criterion, which does not change with time. For example, nearest neighbour or minimum path loss association. UEs can only connect with

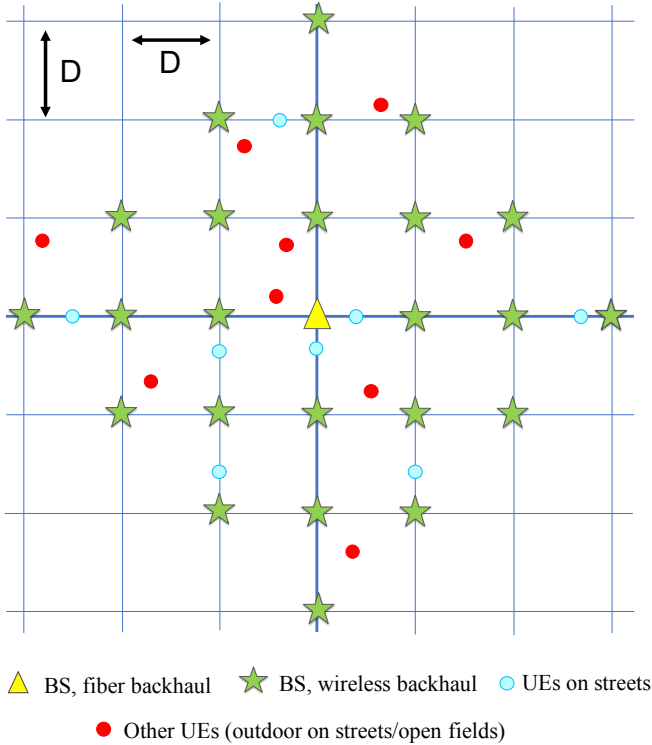


Fig. 1: k -ring model, $k = 3$.

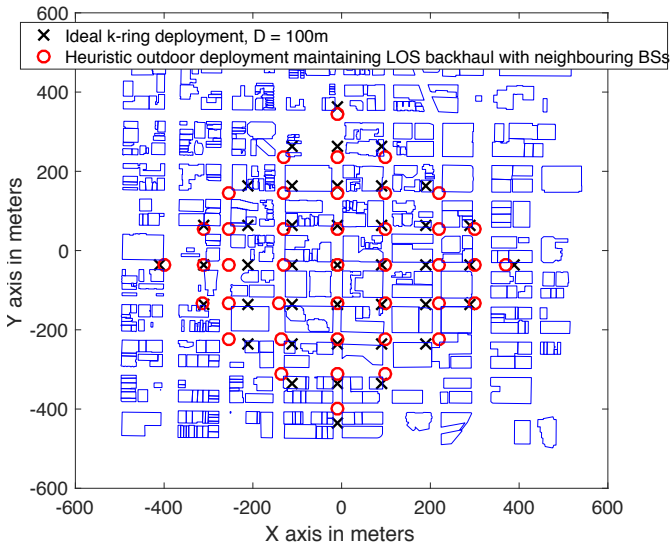


Fig. 2: k -ring model overlaid in an urban area with $D = 100\text{m}$.

BSs along the same street since path loss on links across orthogonal streets can be very high [5], [33]. Number of users connected to a BS at (i, j) is denoted as $w_{i,j}$. A downlink (DL) network is assumed, which implies that the fiber site transmits to all the UEs via relays. BSs and UEs are assumed to employ single stream beamforming. All devices in the network are assumed to be half-duplex.

Routing and traffic model. Time is assumed to be continuous with no explicit slot structure. Total time is 1 unit.

An ordered list of all nodes visited by a UE's data starting from the MBS is called the *route* of that UE. The route includes the UE itself. A *hop* on the route of a UE is a link between adjacent nodes in the route of the UE. It is assumed that *backhauling* (that is BS to BS hops) can happen on links only along a street [5], [33]. Furthermore, it is assumed there is a *unique* route from the fiber site to every UE. Different UEs associated with the same BS can have different routes. For instance, if there are two UEs connected to a BS at $(-1, -1)$, then one of the UE can have a route $(0, 0) \rightarrow (-1, 0) \rightarrow (-1, -1) \rightarrow \text{UE}_1$ and the other UE can have a route $(0, 0) \rightarrow (0, -1) \rightarrow (-1, -1) \rightarrow \text{UE}_2$. Full buffer traffic model is assumed. This implies that given a route of a UE, every BS along the route always has the UE's data to transmit. *Routing strategy* is defined as the collection of routes of all UEs. Given a routing strategy, $f(i, j)$ denotes the effective number of UEs served by (i, j) . That is, $f(i, j) = \sum_{u=1}^U \mathbf{1}\{(i, j) \in \text{route of user } u\}$. Note that $f(0, 0) = U$.

Instantaneous rate and noise-limitedness. Every link (access and backhaul) in the network is associated with a fixed number called instantaneous rate. If a link with instantaneous rate R is activated for time τ , then τR is the data transmitted on that link. Let R_i denote the deterministic instantaneous rate on a backhaul link of length iD for $i = 1, \dots, k$. It is assumed that R_i is decreasing with i . Assumptions on instantaneous access rates will be made in the next section. Note that backhaul links along a street will generally be LOS. Since LOS mmWave links have negligible small scale fading [4], an assumption of deterministic instantaneous rates is justifiable. The analytical results with OAB can be extended for random instantaneous rates for access links, which can incorporate the impact of dynamic blockages, and we will discuss more about this later. Another implicit but important assumption was made above. That is, the instantaneous rates are independent of the *transmission schedules*, that is the set of links activated simultaneously. This is essentially noise-limitedness assumption, which we will extensively validate in Section VI.

Scheduling assumptions. Let L be the total number of links. *Feasible schedules* are defined by a collection of $L \times U$ matrices, called *scheduling matrices*, which are described next. Each entry, $\tau_{l,u}$, in a scheduling matrix indicates fraction of time link l was used to serve data for user u . Here, $0 \leq \tau_{l,u} \leq 1$. Furthermore, since the total time over which optimization is done is 1 unit, the fraction of time every BS is active (that is either transmitting or receiving) is 1. That is, $\sum_{l \in \mathcal{L}_{i,j}} \sum_{u=1}^U \tau_{l,u} \leq 1$, where $\mathcal{L}_{i,j}$ denotes the set of links connected to (i, j) given a routing strategy. Given a routing strategy, there is an extra constraint on the scheduling matrix as follows. If link l is not a hop on route of UE u , $\tau_{l,u} = 0$, $\forall u \in \{1, \dots, U\}$.

III. MAX-MIN END TO END RATE IN k -RING DEPLOYMENT

We want to study what is the maximum value of k that can support a target e2e rate achieved by all UEs. We instead fix a k and find the maximum e2e rate achieved by all UEs. Let

$$\begin{aligned}
& \underset{\mathcal{S}}{\text{maximize}} && \theta_{\mathcal{S}} \\
& \text{subject to} && \theta_{\mathcal{S}} \leq r_l \tau_{l,u}, \forall \text{ hop } l \text{ on the route of user } u, \forall u = 1, \dots, U \\
& && \sum_{l \in \mathcal{L}_{i,j}} \sum_{u=1}^U \tau_{l,u} \leq 1, \forall i, j \in \{0, \pm 1, \dots, \pm k\} \text{ s.t. } |i| + |j| \leq k \\
& && 0 \leq \tau_{l,u} \leq 1, \forall l \in \{1, 2, \dots, L\}, \forall u \in \{1, \dots, U\} \\
& && \tau_{l,u} = 0, \text{ if link } l \text{ is not a hop on route of UE } u, \forall u \in \{1, \dots, U\}
\end{aligned} \tag{1}$$

us define this formally. *Long term rate* of a user u on link l is defined as τR , where R is the instantaneous rate on link l and τ (< 1) is the fraction of time that user u was scheduled on link l . Given a routing strategy and a corresponding scheduling matrix \mathcal{S} , the *e2e rate of UE u* , denoted as $R_u^{\mathcal{S}}$, is the minimum of its long term rate over all hops from the fiber site to the UE.

Definition 1. Given a routing strategy, the max-min rate is defined as $\gamma^* = \max_{\mathcal{S}} \theta_{\mathcal{S}}$, where $\theta_{\mathcal{S}} = \min_{u=1, \dots, U} R_u^{\mathcal{S}}$ with $R_u^{\mathcal{S}}$ being the e2e rate of user u for scheduling matrix \mathcal{S} . Maximizing γ^* considering all routing strategies that are feasible as per the system model in Section II, we obtain the globally optimal max-min rate denoted as R_{e2e}^* .

Given a routing strategy, the max-min rate optimization problem can be restated as in (1), where r_l is the instantaneous rate on link l and \mathcal{S} denotes $L \times U$ matrix with elements $\tau_{l,u}$ for $l = 1, \dots, L$ and $u = 1, \dots, U$. Note that R_{e2e}^* is the maximum of the solution to the above problem over all feasible routing strategies (constraints have been described in Section II).

A. Integrated access backhaul

We first analyze max-min e2e rates for IAB (which corresponds to the above optimization problem) and then turn to the analysis of OAB schemes.

Highway routing. We consider a class of routing strategies called *highway routing*. This is defined as follows. Streets along the X and Y axes are called as *highways*. All UEs associated with a BS at (i, j) have same route from the fiber site to the associated BS. Under a highway routing strategy, the fiber site first transmits data to either $(i, 0)$ or $(0, j)$, whichever is furthest in terms of Manhattan distance, potentially over multiple hops. From $(i, 0)$ or $(0, j)$ the data is then transmitted to the (i, j) along the shortest path in terms of Manhattan distance, potentially over multiple hops. The Manhattan distance of (i, j) from the MBS decreases with every DL hop. If $|i| = |j|$, then the traffic is directed to either $(i, 0)$ or $(0, j)$. However, if $(0, 0) \rightarrow (i, 0) \rightarrow (i, i)$ then $(0, 0) \rightarrow (-i, 0) \rightarrow (-i, -i)$. If there were UL paths, then those would be exactly same as DL paths but in reverse order. Theorem 1 proves the optimality of nearest neighbour highway routing (NNHR) in specific load scenarios and when access rates to all users is the same. We then discuss why NNHR is a good choice in more general load and access rate settings. In Section VI, we empirically observe that NNHR

gives optimal performance in the general UE load scenarios under consideration.

For the first result, all access links are assumed to have a common instantaneous rate R_a (later relaxed). This can be thought as an outcome of power control or just a simplifying assumption.

Theorem 1. Let $w_{0,0} \geq w_{i,j}$ and $w_{i,j} = w_{-i,-j} \forall i, j \in \{0, \pm 1, \dots, \pm k\}$. NNHR is optimal in terms of max-min rates and the optimal rate is given by

$$R_{e2e}^* = \left(\frac{w_{0,0}}{R_a} + \frac{f(0,0) - w_{0,0}}{R_1} \right)^{-1}.$$

A simple hierarchical distributed scheduler that employs integrated access-backhaul, given in Algorithm 1, achieves the max-min optimal rate.

Proof. See Appendix A. \square

Although the assumptions in Theorem 1 are idealistic, it gives an intuition that NNHR can be a good choice when the *bottleneck node* in the network is the fiber site and the effective load on the fiber site is well balanced in all four directions. A *bottleneck node* is formally defined as the node that has at least one link that is always active in order to attain the max-min rates. Also since the derived formula is simple, it offers a quick feasibility check for what is the maximum k that supports a target rate. See Section IV-A for a related discussion.

NNHR may not be desirable in all possible load conditions. However, since having dynamic routing requires exchange of control signals and a more complex system design, it would be desirable to design a system wherein some static routing always gives a reasonable performance. In order to do this network planning, which includes deciding how many antennas should be employed at different BSs in the k -ring deployment or their transmit powers, can play an important role. We now provide guidelines on network planning so that NNHR is justifiable in more general load scenarios.

If the BSs on the highways have much larger antenna gains than the non-highway relays then irrespective of the load it will be beneficial for the relays to employ the highway routing strategies since the highways links have much larger capacity to carry traffic than the non-highway links. We demonstrate this through a quick example. The relay on bottom left corner can transmit towards the fiber site (denoted by the triangle) over two shortest nearest neighbour paths - transmitting to the relay above itself or transmitting to the relay on its right. To do load balancing, let it transmit x fraction of its data to the

Algorithm 1 Theorem 1 scheduler

-
- 1: Denote \mathcal{S}_r as the set of BSs in ring r , where $r = 0, \dots, k$. Ring r implying distance to $(0, 0)$ is rD . Denote by $|\mathcal{S}_r|$ as the cardinality of the set. Total scheduling time is 1 unit.
 - 2: **for** $r = 0 : k$ **do**
 - 3: **if** $r = 0$ **then**
 - 4: The MBS reserves $\frac{w_{0,0}\gamma^*}{R_a}$ fraction of time for access and rest for backhaul.
 - 5: The MBS equally divides the access (backhaul) time frame amongst respective users that need to be served over access (backhaul) links.
 - 6: **else**
 - 7: **for** $q = 1 : |\mathcal{S}_r|$ **do**
 - 8: Let (i, j) be the BS indexed by q . The BS listens to its parent for backhaul for $\frac{f(i,j)\gamma^*}{R_1}$ fraction of time. This is reserved by its parent already in previous for-loop iteration over r . Whenever the BS at (i, j) is not listening, it reserves $\frac{w_{i,j}\gamma^*}{R_a}$ fraction of time for serving access and $\frac{\gamma^*(f(i,j)-w_{i,j})}{R_1}$ for transmitting on backhaul links away from the MBS. In the remaining time, which is non-negative, it stays silent.
 - 9: The BS equally divides the access (backhaul) time frame amongst respective users that need to be served over access (backhaul) links.
 - 10: **end for**
 - 11: **end if**
 - 12: **end for**
-

relay above itself (route 1) and $1-x$ fraction of its data to the relay on the right (route 2). Let γw be the DL rate achieved by each relay in Fig. 3 with relay specific weights w (can be interpreted as number of UEs) written in the square boxes, and we want to maximize γ . Since there are two routes from the relay to fiber site, we need a new definition for the e2e rate of the relay. The e2e rate is γw if the long term rate on each of the hops over route 1 is $x\gamma w$ and the long term rate on each of the hops over route 2 is $(1-x)\gamma w$. Similar to the proof of Theorem 1, the following set of inequalities need to be satisfied. $\gamma \left(\frac{n+4}{R_1} + \frac{n+1+x}{R_1} + \frac{1+1-x}{R_2} \right) \leq 1$, $\gamma \left(\frac{x}{R_2} + \frac{1-x}{R_3} \right) \leq 1$, $\gamma \left(\frac{n+1+x}{R_1} + \frac{n}{R_2} + \frac{x}{R_2} \right) \leq 1$, $\gamma \left(\frac{n}{R_2} \right) \leq 1$, $\gamma \left(\frac{1+1-x}{R_2} + \frac{1-x}{R_3} \right) \leq 1$, and $\gamma \left(\frac{n+4}{R_1} \right) \leq 1$. If R_1 and R_2 are large enough compared to R_3 for a fixed n , then the bottleneck inequality will be $\gamma < R_3/(1-x)$. The optimal choice for x would be closer to 1 in order to maximize the upper bound on γ . As we have seen from Theorem 1, it is possible to construct a scheduling scheme that achieves the upper bound obtained from the inequalities written above. This motivates that when the relays on highways in k -ring deployment are made to have larger antenna gains than the non-highway relays, then the optimal routing paths will tend to be similar to NNHR strategies. We benchmark the performance of NNHR with theoretically optimal nearest neighbour routing (NNR) using the solution in [28] in the numerical results section for general load scenarios.

We now generalize the previous theorem for general load and unequal but deterministic instantaneous access rates to users. For simplicity of exposition, let us number the BSs in the network from 0 to $2k(k+1)$. BS index 0 corresponds to the MBS. With some abuse of notation $f(i)$ now denotes effective load on BS i (number of UEs with the BS i on its route) with new indexing under some routing strategy. Let us also number the users from 1 to $f(0)$ in ascending order of the index of their corresponding serving BS. $R_{a,u}$ denotes instantaneous

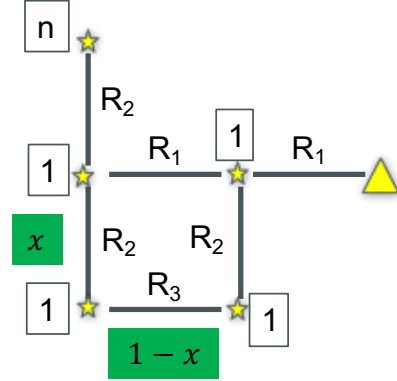


Fig. 3: Justifying highway routing through an example.

access rates of users for $u = 1, \dots, f(0)$.

Theorem 2. Under a given nearest neighbour routing strategy that determines the values of $f(i)$, $\forall i = 1, \dots, 2k(k+1)$, $\gamma^* = \max_{\mathcal{S}} \min_u R_u^S = \left(\max_{i \in \{0, \dots, 2k(k+1)\}} \mathbf{c}_i^T \mathbf{b} \right)^{-1}$, where \mathcal{S} is restricted to all feasible scheduling matrices given the routing strategy,

$$\mathbf{c}_i = \text{sum} \left(\mathbf{I}_{f(0)+1}, \sum_{r=0}^{i-1} w_r, \sum_{t=0}^i w_t \right) + (2f(i) - w_i) \mathbf{e}_{f(0)+1}, \forall i \neq 0,$$

$$\mathbf{c}_0 = \text{sum} (\mathbf{I}_{f(0)+1}, 0, w_0) + (f(0) - w_0) \mathbf{e}_{f(0)+1},$$

where \mathbf{e}_j represents the j^{th} column of identity matrix of dimension $f(0) + 1$ and $\text{sum} (\mathbf{I}_{f(0)+1}, l, u) = \sum_{j=l+1}^u \mathbf{e}_j$. Here,

$$\mathbf{b} = \left[\frac{1}{R_{a,0}} \quad \frac{1}{R_{a,1}} \quad \dots \quad \frac{1}{R_{a,f(0)}} \quad \frac{1}{R_1} \right]^T,$$

where $R_{a,i}$ is the access rate to i^{th} user.

Proof. If γ is a minimum rate achieved by all users, then for BS with index i the following inequality should be satisfied.

$$\gamma \left(\sum_{t=l_i+1}^{l_i+w_i} \frac{1}{R_{a,t}} + \frac{f(i) - w_i}{R_1} + \frac{\mathbb{1}(i \neq 0)f(i)}{R_1} \right) \leq 1,$$

$\forall i = 0, \dots, 2k(k+1)$, where $l_i = \sum_{r=0}^{i-1} w_r$ ensures that the indices from l_i+1 to l_i+w_i correspond to UEs associated with BS i . This inequality can be written as $\gamma \mathbf{c}_i^T \mathbf{b} \leq 1$. To justify that the upper bound on max-min rate given by $\gamma^* = \frac{1}{\max_i \mathbf{c}_i^T \mathbf{b}}$, the following scheduler is sufficient. The MBS first allocates $\frac{(f(0)-w_0)\gamma^*}{R_1}$ fraction of time for backhaul and equally divides the time amongst the $f(0) - w_0$ users which are eventually served over the backhaul links connected to the MBS. The MBS allocates $\gamma^*/R_{a,t}$ fraction of time for user t connected to MBS, where $t = 1, \dots, w_0$. Then in the time when a relay in ring 1 is not scheduled by the MBS, it allocates $\frac{(f(i)-w_i)\gamma^*}{R_1}$ fraction of time for serving over backhaul links away from the fiber site, which is equally divided for transmitting data of each of the $f(i) - w_i$ users. The relay allocates $\gamma^*/R_{a,t}$ fraction of time for user t connected to it, where $t = 1, \dots, w_i$. This process continues hierarchically for all relays in the k -ring deployment. \square

Now, we extend the result in Theorem 2 to full duplex BSs. Instead of the required fraction of time for reception plus transmission being ≤ 1 for every BS, we now have two separate inequalities per BS – one for transmission time and one for reception time. Since there will be self-interference at each relay the access rates and backhaul rates will be different than in Theorem 2. Let access rates to users under full duplex relaying be $R_{a,i}^f \leq R_{a,i}$ and the single hop backhaul rate be $R_1^f \leq R_1$. Although the system model set up in Section II was for DL, all the relevant definitions can be extended for UL as well. We now consider a scenario when there are some UL and some DL UEs. Note that a UE cannot be both UL and DL. Let \mathcal{U}_{DL} and \mathcal{U}_{UL} be the set of indices of downlink (DL) and uplink (UL) UEs. Let w_i^{DL} and w_i^{UL} denote the number of DL and UL UEs connected to BS i . Similarly, $f^{DL}(i)$ and $f^{UL}(i)$ corresponds to effective DL and UL load on BS indexed by i .

Theorem 3. *Considering full duplex BSs, and under a given nearest neighbour routing strategy that determines the values of $f^{DL}(i)$ and $f^{UL}(i)$, $\forall i = 1, \dots, 2k(k+1)$, $\gamma^* = \max_S \min_u R_u^S = \min(\gamma_{tx}, \gamma_{rx})$, where S is restricted to all feasible scheduling matrices given the routing strategy,*

$$\gamma_{tx} = \left(\max_{i \in \{0, \dots, 2k(k+1)\}} \mathbf{c}_{tx,i}^T \mathbf{b}_f \right)^{-1}$$

and

$$\gamma_{rx} = \left(\max_{i \in \{0, \dots, 2k(k+1)\}} \mathbf{c}_{rx,i}^T \mathbf{b}_f \right)^{-1}.$$

Here,

$$\mathbf{b}_f = \left[\frac{1}{R_{a,0}^f} \quad \frac{1}{R_{a,1}^f} \quad \dots \quad \frac{1}{R_{a,f(0)}^f} \quad \frac{1}{R_1^f} \right]^T,$$

$$\begin{aligned} \mathbf{c}_{tx,i} &= \text{sum}^{\text{DL}} \left(\mathbf{I}_{f(0)+1}, \sum_{k=0}^{i-1} w_k, \sum_{k=0}^i w_k \right) + \\ &\quad (f(i) - w_i^{\text{DL}}) \mathbf{e}_{f(0)+1}, \quad \forall i \neq 0, \\ \mathbf{c}_{tx,0} &= \text{sum}^{\text{DL}} (\mathbf{I}_{f(0)+1}, 0, w_0) + (f^{\text{DL}}(0) - w_0^{\text{DL}}) \mathbf{e}_{f(0)+1}, \\ \text{sum}^{\text{DL}} (\mathbf{I}_{f(0)+1}, l, u) &= \sum_{j=l+1}^u \mathbf{e}_j \mathbb{1}(\text{UE } j \text{ is DL}), \end{aligned}$$

where \mathbf{e}_j represents the j^{th} column of identity matrix of dimension $f(0)+1$. $\mathbf{c}_{rx,i}$ is same as $\mathbf{c}_{tx,i}$ but with superscript DL replaced by UL in all places.

The proof of Theorem 3 is similar to that of Theorem 2. With these general formulae for IAB, we next turn our attention to the analysis of a couple of OAB schemes.

B. Orthogonal access backhaul

Max-min optimization with IAB may face difficulties for practical implementation, owing to the need to know global information of load and access rates for solving the optimization problem. The OAB schemes discussed here are potentially simpler to implement. Let ζ be the fraction of resources reserved for access and rest are reserved for backhaul. We now perform optimization only over entries of the scheduling matrices for backhaul links. Every BS is assumed to divide the access time equally amongst all UEs directly associated with it. Furthermore, now all UEs associated with a BS have same route from the fiber site to the associated BS.

If a backhaul link with instantaneous rate R is activated for τ fraction of time to serve all UEs associated with a relay, then *long term backhaul rate of a relay on a link* is defined as τR . Furthermore, *e2e backhaul rate of a relay* is defined as minimum of long term backhaul rate of the relay over each hop from the fiber site to the relay.

We first consider a simple OAB scheme wherein equal e2e rate is offered to each relay. As this scheme does not optimize the rates based on load per BS, there will be some over-utilized and some under-utilized BSs. This issue, however, can be addressed by enabling dual connectivity which we will study in the next section. For simplicity of exposition, assume DL backhauling. The analysis holds for a mix of DL and UL backhauling since instantaneous link rates on backhaul do not change for UL and DL.

Theorem 4. *If all relays are offered an equal e2e backhaul rate, say γ . Maximizing γ over all scheduling matrices with OAB, we get the optimal e2e backhaul rate is $\frac{(1-\zeta)R_1}{2k(k+1)}$ and NNHR is optimal. Furthermore, e2e rate for any user connected to some BS at (i, j) is given by $\frac{1}{w_{i,j}} \min(\zeta R_a, \frac{(1-\zeta)R_1}{2k(k+1)})$, assuming every BS divides the access and backhaul time equally amongst the users directly associated with that BS.*

Proof. Let γ be the maximum long term rate offered to each relay assuming NNHR. Then the following should be satisfied. γ/R_1 is the minimum fraction of resources that are allocated for backhauling to each of the $2k(k+1)$ relays by the MBS. Thus, $\gamma(2k(k+1))/R_1 \leq (1-\zeta)$. Let $f(i, j) - 1$ represent total

number of relays served by (i, j) . The following inequalities should also hold. $\gamma \left(\frac{f(i,j)-1}{R_1} + \frac{f(i,j)}{R_1} \right) \leq 1 - \zeta$, for all $(i, j) \neq (0, 0)$. Here, $\gamma f(i, j)/R_1$ is the fraction of time for relaying data to (i, j) from the fiber site. $\frac{f(i,j)-1}{R_1}$ is the fraction of time for relaying data from (i, j) to the BSs away from the fiber site. Since $2f(i, j) - 1 < 2k(k+1)$, which holds because $f(i, j) = f(-i, -j)$ considering NNHR, the least upper bound on γ is $\gamma \leq (1 - \zeta)R_1/2k(k+1)$. This is achieved by using a scheduler similar to Algorithm 1. The main difference is that R_a is set to ∞ , which makes time allocated for access equal to zero, and $w_{i,j} = 1$ making $f(i, j)$ as the effective number of relays served by (i, j) including itself.

A non-NNHR scheme cannot offer rates higher than $(1 - \zeta)R_1/2k(k+1)$ as the fiber site will always have to support at least $2k(k+1)$ relays, irrespective of the routing scheme. This proves $\gamma = (1 - \zeta)R_1/2k(k+1)$. By definition, the e2e rate for a user is the minimum of its access long term rate and e2e backhaul rate. Consider a UE connected to (i, j) . Since backhaul rate to (i, j) is equally divided amongst all $w_{i,j}$ users, the e2e backhaul rate of the UE is $\frac{(1-\zeta)R_1}{w_{i,j}2k(k+1)}$. Long term access rate of the UE is $\zeta R_a/w_{i,j}$, since each user connected to a relay receives equal fraction of time for access. Thus, the e2e rate for the user is given by $\frac{1}{w_{i,j}} \min(\zeta R_a, \frac{(1-\zeta)R_1}{2k(k+1)})$. \square

Corollary 1. *If $w_{i,j} = w_{-i,-j}$ and $w_{0,0} \geq w_{i,j}$ and access rates to all UEs are given by R_a , there exists an OAB strategy that performs as good as IAB in terms of max-min rates.*

Proof. Consider the following OAB scheme. ζ is the fraction of access resources (also called as slots) and $1 - \zeta$ is the fraction of backhaul slots. Within the backhaul slots, target long term rate to each relay is $\gamma w_{i,j}$, for all i, j . Resources are allocated to maximize γ .

Assuming NNHR, similar inequalities as (2) and (3) can be written to find an upper bound on γ with the following differences. Since access resources are orthogonal from backhaul resources, the terms of the form $w_{i,j}/R_a$ are not present as in (2) and (3) but the rest of the terms in those equations remain the same since e2e backhaul rate per relay is $\gamma w_{i,j}$. Thus, it is easy to see that $\gamma \leq \frac{(1-\zeta)R_1}{f(0,0)-w_{0,0}}$. Achieving the upper bound is possible employing a scheduler same as Algorithm 1 with the following difference. Set $R_a \rightarrow \infty$ to make sure there are no access slots allocated in the backhaul resource blocks. Optimality of NNHR is argued exactly as in proof of Theorem 1. This implies maximum achievable $\gamma = \frac{(1-\zeta)R_1}{f(0,0)-w_{0,0}}$.

Thus, with the OAB scheme under consideration the e2e rate for a user connected to a BS at (i, j) is given by $\min(\frac{\zeta R_a}{w_{i,j}}, \frac{(1-\zeta)R_1}{f(0,0)-w_{0,0}})$, assuming round robin scheduling done by (i, j) amongst $w_{i,j}$ UEs for access and that the e2e backhaul rate to (i, j) was equally divided amongst all $w_{i,j}$ UEs. Minimum e2e rate corresponds to $i = j = 0$. Maximizing minimum e2e rate over ζ , it is found that the max-min rate equals $\left(\frac{w_{0,0}}{R_a} + \frac{f(0,0)-w_{0,0}}{R_1} \right)^{-1}$, same as Theorem 1. \square

End-to-end backhaul rate with the OAB scheme described in the proof of Corollary 1 can be analyzed in general load scenario, like in Theorem 2. In this case, the e2e backhaul rate

is exactly same as that in Theorem 2 but replacing $1/R_{a,u}$ by 0 in the definition of vector \mathbf{b} . If long term rate of a UE on a link is defined as $\lim_{t \rightarrow \infty} \frac{1}{T} \int_0^{\tau T} X(t) dt$, where τ is the fraction of time the link was active to serve the UE and $X(t)$ is a stationary ergodic random process and denotes the instantaneous rate of the link as a function of time, then using ergodic theorem the e2e rates in Theorem 4 can be extended even when access rates are random variables (backhaul rates are still deterministic) by replacing R_a with $\mathbb{E}[R_a]$.

IV. EXAMPLE APPLICATIONS OF THE ANALYSIS

In this section, we discuss some simple use-cases of our analysis.

A. 5G Networks with Minimum Rate of 100 Mbps

Deploying a new cellular network operating at mmWave involves significant cost and time overheads. Thus, it does not make sense if the deployed mmWave network offers only marginal gains over existing 4G networks. A minimum 100 Mbps per UE target has been set for 5G networks operating at mmWave frequencies. The analysis can be used to evaluate feasibility of potential BS or UE deployments for 5G networks.

1) *Minimum number of rings required to get 100 Mbps rates:* A closed-form expression for maximum k that supports 100 Mbps per UE can be obtained in simple settings like Theorem 1.

Corollary 2. *The maximum k that can still meet the max-min target rate of γ_{target} is given by $k \leq \frac{\sqrt{1+2R_1 \left(\frac{1}{w\gamma_{\text{target}}} - \frac{1}{R_a} \right)} - 1}{2}$, if all relays have equal load w and $\gamma_{\text{target}} > \frac{R_a}{w}$.*

Proof. The max-min rate is given by $\gamma^* = \frac{1}{w} \left(\frac{1}{R_a} + \frac{2k(k+1)}{R_1} \right)^{-1}$. Rearranging and solving the quadratic equation we get the result by using $\gamma^* \geq \gamma_{\text{target}}$. \square

2) *Soft max-min:* Strictly maximizing the minimum rate in a mmWave system may lead to very poor e2e rates achieved by all UEs if a few of the UEs have very poor spectral efficiency, e.g. they are severely blocked by surrounding objects. Thus, it is practically beneficial to softly optimize the max-min rates. Here, we demonstrate a possible procedure. UEs that have very poor spectral efficiency, denoted as “bad UEs”, are placed with pseudo UEs for finding max-min rates. The pseudo UEs fake a higher signal to interference plus noise ratio (SINR) for the corresponding “bad UEs”. This allows the rest of the “good UEs” to have much better rates after max-min optimization is performed. Essentially, these “bad UEs” sacrifice themselves for the benefit of the whole. In a practical 5G system, such UEs would soon switch to a sub-6GHz legacy band to maintain a minimum performance level.

B. Analyzing performance of dual-connectivity.

Multi-connectivity, wherein a UE connects to multiple BSs on the same or different bands, can counteract dynamic blocking in mmWave cellular. For self-backhauled networks, dual connectivity has another advantage to smooth out the load

imbalance across all BSs. This can make resource allocation simpler in self-backhauled networks since employing equal rate per relay OAB is much simpler than IAB.

Here, we look at a specific implementation of dual-connectivity (DC). OAB is assumed with ζ fraction of resources for access. DL UEs are assumed. Optimization is done to offer equal backhaul rates per relay. Consider a user connected to two BSs offering least path loss. Consider a user connected to relays at (i, j) and $(i - 1, j)$. Let the distance from the two BSs be x and $y (< x)$, respectively. It is assumed that the UE has at least two RF chains so that it can receive signals from both connected BSs simultaneously. $R_a(x)$ is the access rate to the user from BS at (i, j) and $R_a(y)$ is the access rate from BS at $(i - 1, j)$. Let R_{single} and R_{dual} be the rates of the user under single connectivity (SC) and DC. Using Theorem 4, $R_{single} = \frac{1}{w_{i,j}} \min\left(\zeta R_a(x), \frac{(1-\zeta)R_1}{2k(k+1)}\right)$. Considering DC, $r_1 = \frac{1}{w_{i,j}} \min\left(\zeta R_a(x), \frac{(1-\zeta)R_1}{2k(k+1)}\right)$ and $r_2 = \frac{1}{w_{i-1,j}} \min\left(\zeta R_a(y), \frac{(1-\zeta)R_1}{2k(k+1)}\right)$ are e2e rates of the UE over its two connections, where $w_{i,j} (\geq w_{i-1,j})$ is the new load on (i, j) after dual connectivity. Thus, R_{dual} can be defined as $R_{dual} = r_1 + r_2$, where additivity arises from the interpretation of e2e rate as total data transmitted from source to destination in 1 unit time. Following remarks describe how to compute the access and backhaul rates.

Remark 1 (Computing access rates). $R_a(x) = W \min(\log_2(1 + \text{SNR}_a), \text{SE}_{\max})$, where SNR_a is the effective received signal power to noise power ratio and is equal to $\left(\frac{\sigma^2}{P_r} + \frac{1}{\text{SNR}_{\max} N_r}\right)^{-1}$. Here, P_r/σ^2 is the actual signal to noise ratio (SNR) as defined next, and $\text{SNR}_{\max} N_r$ limits the maximum possible received SNR with N_r equal to the number of receiver antennas. A similar model for dampening very high SNR due to device imperfections is common in the industry, e.g. see the Qualcomm paper [34]. It can be derived by modeling a virtual amplify-and-forward transmission hop within the receiving device, which leads to effective SNR being half of the harmonic mean of the actual and maximum SNR [35, (4)]. Note that for large $\text{SNR}_{\max} N_r$, the effective SNR is close to P_r/σ^2 . However, if P_r/σ^2 is itself very large, then the SNR cannot exceed $\text{SNR}_{\max} N_r$. Note that SE_{\max} is the limit on maximum spectral efficiency, which is related to modulation and coding employed by the receiver. Here, $P_r = \left(\frac{\lambda}{4\pi}\right)^2 \Upsilon \text{P}_{\text{NBS}} \text{N}_{\text{UE}} x^{-\alpha}$, where P is the transmit power, σ^2 is the noise power, W is the bandwidth, N_{BS} and N_{UE} are the number of antennas at the BS and UE, λ is the wavelength in meters, Υ is the blockage dependent correction factor [36], and α is the blockage dependent path loss exponent (PLE). If the link is LOS, then $\alpha = \alpha_l$ and $\Upsilon = 1$. If the link is NLOS, then $\alpha = \alpha_n$ and $\Upsilon = \Upsilon_n \ll 1$.

Remark 2 (Computing backhaul rate). $R_1 = W \min(\log_2(1 + \text{SNR}_b), \text{SE}_{\max})$, where SNR_b is half of the harmonic mean of $\frac{(\lambda/4\pi)^2 \text{P}_{\text{NBS}} D^{-\alpha_l}}{\sigma^2}$ and $\text{SNR}_{\max} \text{N}_{\text{BS}}$.

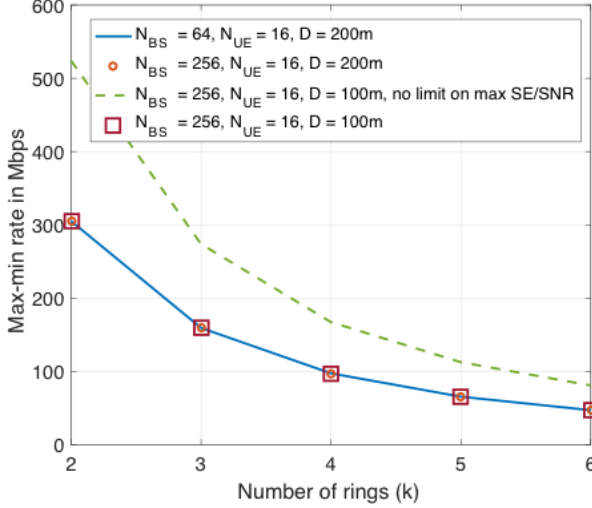
TABLE I: Default numerical parameters

No-ta-tion	Param-eter(s)	Value(s) if appli-cable	No-ta-tion	Param-eter(s)	Value(s) if applicable
f_c	Carrier frequency	28 GHz [1]	W	Total bandwidth	800 MHz [1]
P_d	BS transmit power	30 dBm [1]	P_u	UE transmit power	23 dBm [1]
η	Fraction DL UEs	1	σ^2	Noise power	$-174 + 10 \log_{10}(W) + 10$ dBm
α_l	LOS PLE	2 [37]	α_n	NLOS PLE	3.4 [37]
N_{BS}	BS antennas	64 [32]	N_{UE}	UE antennas	16 [32]
D	ISD	200m (Fig. 2)	k	Number of rings	3
Υ_n	Correc-tion factor	-5dB [27], [36]	SE_{\max}	maximum spectral efficiency	10 bps/Hz [38]

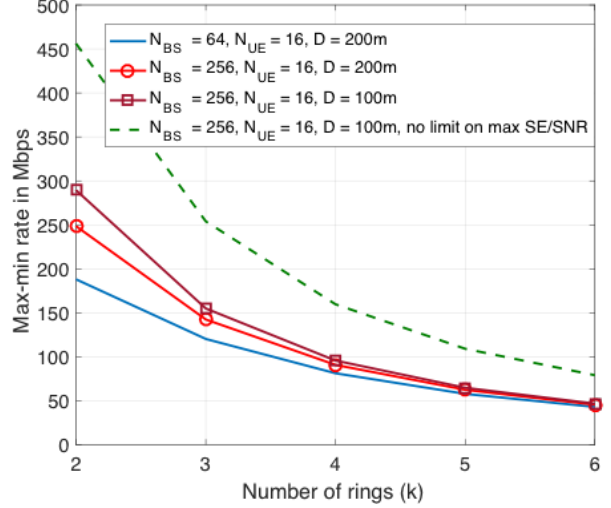
V. NUMERICAL RESULTS AND DESIGN GUIDELINES BASED ON ANALYSIS

In this section, we evaluate the derived formulae to explore system design insights for multi-hop mmWave cellular networks. In the next section, the main analytical assumption – noise-limitedness – will be validated. Table I summarizes key parameters which are fixed throughout the numerical study, unless specified otherwise. NNHR is assumed, unless specified otherwise. We choose $\text{SNR}_{\max} = 16$ dB, so that the maximum received SNR at UEs equals 28 dB considering 16 antennas, which is close to the 30dB value in [34]. For backhaul links, the maximum received SNR is 34 dB considering 64 antennas. For 5G-NR, it is possible to support up to 1024 QAM [38] and thus $\text{SE}_{\max} = 10$ bps/Hz is chosen.

Fall in throughput with number of rings. To understand the fall in throughput with number of rings, we consider 2 worst case UEs per BS located at a distance $D/2$ on the streets. LOS access and all DL UEs is assumed. Fig. 4(a) shows the fall in throughput with number of rings. It is surprising to note that it is possible to achieve minimum 100 Mbps per UE with even a 4 ring deployment, which covers an area of 1.1×1.1 km² and supports 40 relays per fiber site. Having a larger N_{BS} hardly changes the rate as the network is backhaul limited with backhaul links operating at SE_{\max} . Decreasing D to 100 meters also does not change the rates. As per Corollary 2, throughput decays as $\frac{1}{w} \left(\frac{1}{R_a} + \frac{2k(k+1)}{R_1}\right)^{-1}$. Since we consider LOS UEs, R_a is already saturated by SNR_{\max} for $D = 200$ m. Also, R_b is limited by SE_{\max} and does not change by decreasing D . However, note that 2 UEs per BS with $D = 100$ m itself supports 4x higher user density than for $D = 200$ m. If there were no limit on spectral efficiency or SNR, then even up to $k = 6$ with $D = 100$ m, that covers an area of 850×850 m², can be supported with user density of 200 UEs/km². This result motivates supporting higher order modulations and enabling the use MIMO on backhaul links to increase the spectral efficiency for enabling the support of higher load per BS or larger value of k for the same target per user rate.



(a) 2 LOS UEs per BS located at 100 m from the serving BS.



(b) 2 NLOS UEs per BS located at 100 m from the serving BS.

Fig. 4: Fall in throughput with k .

As can be seen in Fig. 4(a), throughput decays quickly with k as the networks are backhaul limited. For large values of k , when the $1/R_a$ term is negligible, throughput decays by a factor of $k/(k+2)$ as k increments by 1. The $1/R_a$ factor makes throughput decay slightly slower than above for smaller values of k . More specifically, if one fits function α/k^β to the plot for $N_{BS} = 64$ and $N_{UE} = 16$, then $\beta = 1.6$. The decay is slower in access limited networks, when $1/R_a$ term is non-negligible. This can be observed from Fig. 4(b), which reproduces the scenarios in Fig. 4(a) but with NLOS UEs. Note that up to 3 rings can be supported even with NLOS UEs.

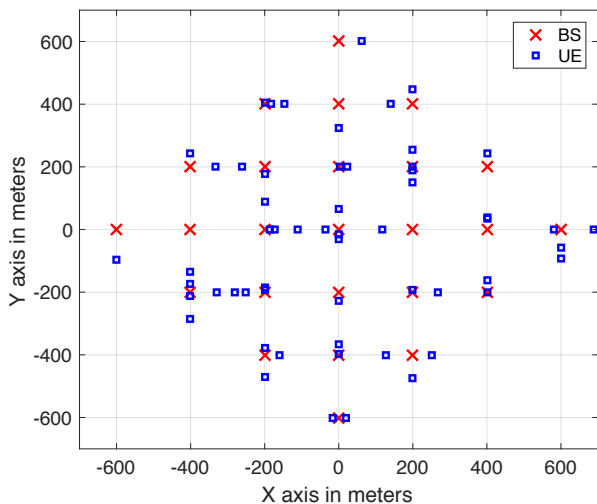
We now consider a more general UE deployment setup as shown in Fig. 5(a). On an average there are 2 UEs per BS in the 3-ring deployment. A random realization of LOS/NLOS states for UE to/from BS links was generated considering 50% probability of being LOS within a distance of 200m. Minimum path loss association is done. For the realization considered, 55% UEs connected to LOS BSs. Also by default $\eta = 0.5$, that is about 50% UEs are DL and rest are UL. Spectral efficiency (SE) has a minimum limit of 0.02 bps/Hz below which rate is 0.

Impact of Full Duplex Relays. Fig. 5(b) shows the comparison of full and half duplex relaying. X axis is the self-interference (SI) introduced by full duplexing and Y axis plots the optimal rates in Mbps. We consider soft max-min optimization, introduced in Section IV-A, wherein 10% of bad UEs are replaced with pseudo UEs that fake an arbitrarily large rate. We consider soft max-min since we observe that considering max-min optimization in the considered setup leads to a conclusion that full duplexing can provide higher rates than half duplex only if SI is less than -110 dB, which is impractical to achieve as per state of the art prototypes [39]. Fig. 5(b) explores scenarios wherein larger SI can be tolerated. Even with soft max-min optimization, significant gains with

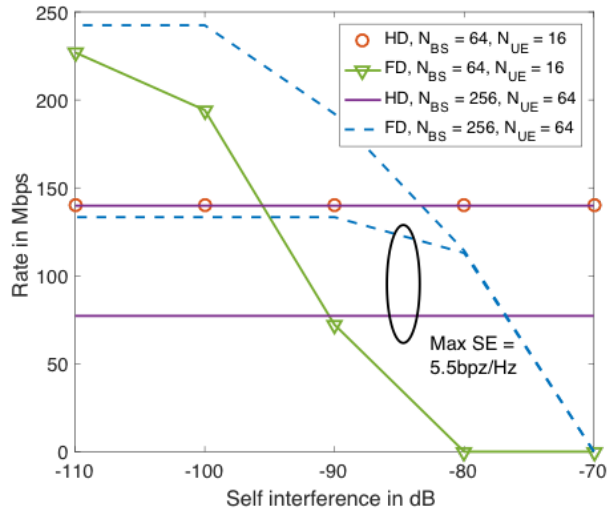
full duplexing are observed for the default setup only if $SI < -100$ dB. Fig. 5(b) shows that considering larger antenna gains at the BSs and UEs helps increase the requirement of maximum tolerated SI to -90 dB. Considering a maximum spectral efficiency of 5.5 bps/Hz further increases the tolerance of SI to -80 dB, which is practical [39]. Note that 5.5bps/Hz corresponds to spectral efficiency with 64 QAM and light coding. Similar values of SE_{max} have been used in prior work [37], [40]. We next turn our attention to understanding if OAB can closely follow the rates obtained using IAB.

OAB versus IAB. The distribution of e2e rates obtained using OAB is compared with IAB in Fig. 6(a). We consider two types of OAB. First allocates equal backhaul rate to each relay (called type 1). Second type offers a backhaul rate $w_{i,j,\gamma}$ to a relay at (i, j) , wherein maximum γ is computed (called type 2). The max-min rates with IAB outperform the rate obtained by more than 60% of UEs with OAB type 1. Although not shown in the plot, varying $\zeta \in (0, 1)$ does not change this insight. However, it is interesting to note that with OAB type 2 it is possible to achieve rates slightly greater than IAB rates for about 85% UEs by choosing $\zeta = 0.15$. This is encouraging for practical implementations since OAB type 2 requires less global information for performing the optimization as compared to IAB.

Dual connectivity versus single connectivity. We conclude our discussion of design insights based on the analysis by evaluating the benefit of DC as described in Section IV-B. Fig. 6(b) plots the rates with SC and DC considering two deployments and OAB type 1. Deployment A is the one in Fig. 5(a), wherein there are about 2 UEs per BS on an average with a load variance of 1.1. Deployment B is not shown for space constraints and has same mean UEs per BS but variance is 2.3. For deployment B, median rates with DC are almost 1.5x higher than SC. Although the load per BS is higher with DC, the load imbalance across BSs is reduced. Since equal

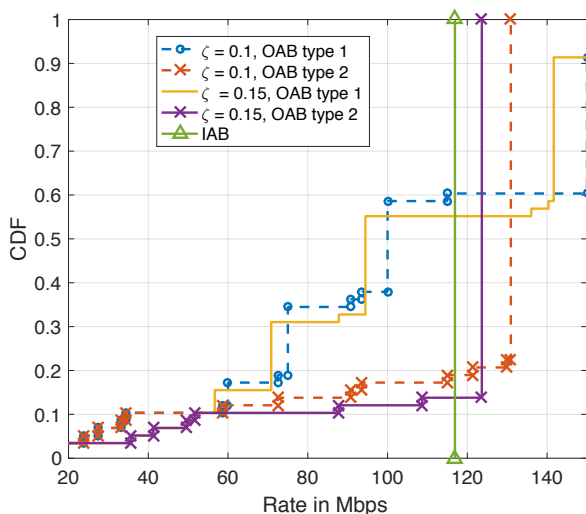


(a) Topology under consideration.

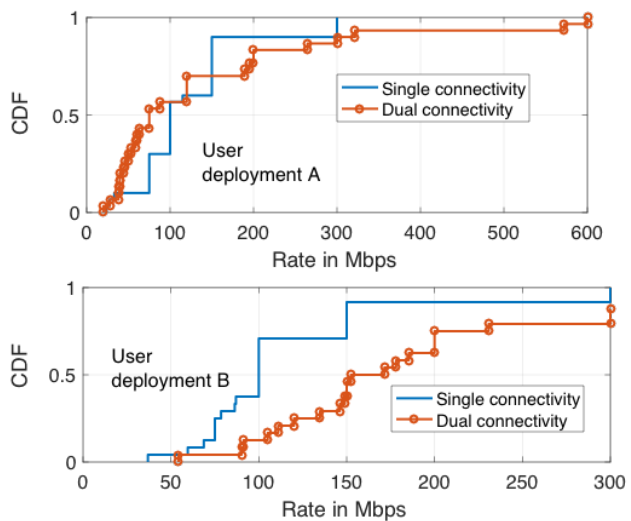


(b) Full versus half duplex relaying with soft max-min.

Fig. 5: Impact of full duplex relaying on max-min rates.



(a) OAB type 2 closely follows IAB.



(b) Impact of dual connectivity on rate.

Fig. 6: OAB vs IAB, and impact of dual connectivity.

backhaul rate per relay is offered, load balancing makes it possible to exploit the underutilized backhaul links. However, note that the rates with DC are roughly similar to SC for deployment A with lower load imbalance of UEs across BSs. We observe that in general the higher the load imbalance with SC, the higher the gain in data rates with DC.

VI. VALIDATION OF NOISE-LIMITEDNESS.

Same default parameters as Table I are used in this section. The goal is to motivate why noise-limited analysis works through a couple of empirical observations. Also, we observe NNHR operates optimally even in more general scenarios than in Theorem 1. We also propose a greedy variant of proportional fair (PF) scheduling for multi-hop networks in

one of the numerical examples that is used to validate noise-limited analysis. This example is also useful to show how the analysis can be used as a benchmarking tool for complex simulators. All UEs are DL.

A. Few bottleneck links helps noise-limitedness.

We compare the max-min rate obtained from our noise-limited analysis with that computed using the linear programming (LP) solution in [28], which jointly optimizes the scheduling and routing. An arbitrary deployment was considered and interference was not neglected in [28]. This, however, lead to a LP formulation with very high numerical complexity as compared to our work. Specifically, if there are L links in

the network one needs to create matrices of the size on the order of 2^L to implement the LP.

Simulation setup. We consider the deployments in Fig. 5(a) and Fig. 7(a) with average loads equal to 2.3 UEs per BS and 1 UE per BS. Searching over all possible routes is not possible using the algorithm in [28] considering that the network in Fig. 5(a) has 25 BSs and 58 UEs. We reduce the search space by considering only NNR (not necessarily highway routing) on the grid. Since listing all scheduling patterns given NNR is itself time and memory intensive (there are 86 valid links in Fig. 5(a) even after reducing the search space for routing and there will be on the order of 2^{86} potential schedules), we do a greedy search to list transmission schedules. Banking on the possible noise-limitedness, we first greedily list 250 transmission schedules that have at least 10 active links still respecting the half duplex constraint, half of them forced to have at least one backhaul link connected to the fiber site. Then we append all transmissions schedules which have 3 links active at a time to make sure the LP has a solution. The greedy schedules were considered to check if after ignoring interference, do the max-min rates improve by using the greedy schedules instead of activating only 3 links at a time.

To model interference, we consider received signal power from interfering transmitters as $P_r = (\lambda/4\pi)^2 P G_t G_r x^{-\alpha}$, where G_t and G_r are random antenna gains and rest of the parameters are defined in Remark 1. All links along same street are LOS and all links across different streets are NLOS. Here, $G_t = G_{\max}$ if the interfering link is pointed exactly towards the receiver and $G_t = G_{\min}$, otherwise. Similarly, $G_r = G_{\max}$ is the receiver under consideration has beam pointed towards the interferer and $G_r = G_{\min}$ otherwise. Note that we have only 4 directions to point in the grid deployment. Here, $G_{\max} \in \{N_{\text{BS}}, N_{\text{UE}}\}$ depending on whether the transmitter or receiver is a BS or UE, and $G_{\min}(\text{dB}) = G_{\max}(\text{dB}) - 25\text{dB}$, where 25 dB is the front to back ratio. Using a spatially consistent path loss model inspired from [5], it was shown in [33] that NLOS interferers on different streets contribute negligibly to total interference in an urban canyon type deployment model. However, we still incorporate interference from NLOS interferers to create worst case scenarios. We assume NLOS interferers always have beams aligned with maximum antenna gain chosen for G_t and G_r . Note that we are not exploiting narrowness of beams from NLOS interferers and thus the interference we consider can be interpreted as worst case.

Comparing max-min rates with and without interference. Table II summarizes the results of max-min rates obtained by running the LP in [28] for different scenarios. Specifically, max-min rates were computed assuming noise-limitedness and considering interference. Also, max-min rates were computed assuming NNHR and without such an assumption. Here, t_1 denotes the fraction of time that the greedy schedules were used, so $1 - t_1$ is the fraction of time 3 links were active at a time. The fraction of time wherein at least one link connected to the fiber site was active is denoted by t_2 .

It is surprising to note that irrespective of whether interference is considered or not, the max-min rates do not change.

TABLE II: Empirical evidence for noise-limitedness and justification of highway routing.

Scenario (Fig. 5(a))	t_1	t_2	Max-min rate (Mbps)	Scenario (Fig. 7(a))	t_1	t_2	Max-min rate (Mbps)
Optimal NNR + interference	0.03	1	137.15	Optimal NNR + interference	0.00	1	304.64
Optimal NNR without interference	0.04	1	137.17	Optimal NNR without interference	0.01	1	304.64
NNHR + interference	0.04	1	137.08	NNHR + interference	0.01	1	304.64
NNHR without interference	0.03	1	137.17	NNHR without interference	0.01	1	304.64

Furthermore, the rates do not change irrespective of whether NNHR or optimal NNR is considered. Also note that the rate corresponding to Fig. 5(a) is exactly same as the IAB rate in Fig. 6(a) using our analysis. Similarly it was confirmed that the max-min rate corresponding to Fig. 7(a) is equal to that from our analytical result in Theorem 2. These observations are explained by noting the values of t_1 . Since $t_1 \ll 1$, most of the schedules used only 3 active links at a time to meet the max-min rates. In other words, the optimal scheduler did not use the transmission schedules with greedy packing. Thus, the interference is negligible in these scenarios. As mentioned in [28] there is no unique solution to the LP and thus the values of t_1 are not unique. The key takeaway, however, is that there exists a solution that achieves max-min rates under the scheduling and routing search space considered with small t_1 . Since $t_2 = 1$, it implies the bottleneck node is the fiber site. This exercise highlights the importance of our noise-limited analysis and also makes a case for near optimality of NNHR.

Similar observation highlighting noise-limitedness due to interference aware schedulers were reported in [24], [28]. If one comes across a deployment and traffic scenario wherein the rates with NNHR are much lower than optimal NNR, then the methodology discussed in Section III-A to increase the antenna gains on highway relays can be attempted. Our code for implementing the LP in [28] is available at [41].

Remark 3. Since our analytical results with NNHR give the same rate as that obtained by employing the LP in [28], the results for NNHR in Table II are accurate in spite of a small search space. Furthermore, increasing the number of greedy schedules to 1800 did not change the result for the case of NNR without interference, making us confident on the near optimality of NNHR in the scenario considered.

Noise-limitedness is observed in the validation results since the scheduler is intelligent to pick the right balance of choosing different combination of 3 active links at a time to avoid interference on the bottleneck links. Developing practical schedulers which identify and protect the bottleneck links

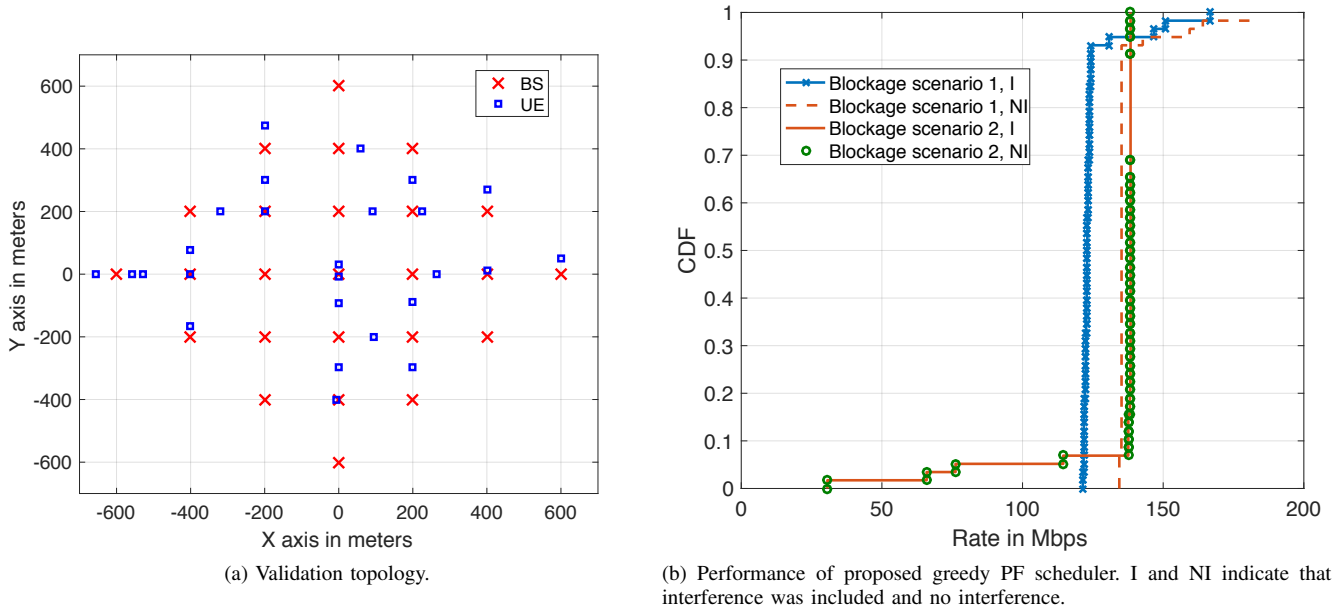


Fig. 7: Validation plots.

from interference is one avenue of further research. We now report another interesting observation that shows that even if schedulers are not interference-aware, noise-limited analysis can still provide accurate estimates of achievable rates in spite of interference.

B. Blockage effects and directionality helps noise-limitedness.

In this section, we show that the blockage effects at mmWave along with directionality of transmissions in the k -ring deployment can enable noise-limited analysis even if the scheduler does not explicitly protect interference on bottleneck links. We now assume that transmitters on different streets than the receiver have negligible interference, since the path loss exponent can be as large as 10 for the NLOS segments of such links [5], [33]. We simulate the performance of the deployment in Fig. 5(a) using NNHR and a greedy variant of the popular backpressure scheduler with congestion control on the first hop as in [42]. We call this as the greedy PF scheduler and it greatly simplifies the implementation of the GBD algorithm in Section I-C of [42]. We choose this particular baseline algorithm, since it emulates PF for multi-hop networks with the utility function in Section I-C of [42] being $U(x) = \log(x)$, which has been a popular paradigm for employing in 4G cellular networks. Another reason for choosing this scheduler is that the discussion in this work is limited to full buffer assumption until now, and considering a scheduler that works for time varying traffic is desirable. This would pave a way for evaluating packet latencies in multi-hop mmWave networks. However, in this section we assume the fiber site always has infinite backlogged data for all UEs. Each BS in the k -ring deployment now represents a queue with multiple traffic flows, each UE representing a flow. Here, we simulate the queueing network for a reasonably long time to understand whether directionality and blockage

effects helps keep the network noise-limited even with the proposed simplified scheduler which is not interference-aware. Understanding the stability of the queueing network is an avenue of future research.

Assuming NNHR, scheduling is done as follows. We assign priority of scheduling a particular flow on a particular link by the *backpressure* metric, that is product of noise-limited estimate of the instantaneous rate on the link times difference in queue length at the source and destination for the flow on that link. For full buffer traffic, the queue length at source is infinite, which is why the backpressure metric needs modification on the first hop. Congestion control is done as discussed in [42] to emulate PF scheduling and the priority metric for flow f on link i , which corresponds to first hop for flow f , is $r_i(t) \left(\frac{1}{cR_i^f(t)} - q_i^f(t) \right)$, where $r_i(t)$ is the noise-limited instantaneous rate of link i at time t , q_i^f is the queue length for flow f at the destination of link i and c is the congestion control parameter (set to be 10^{-14} to create high backpressure on the first hop for all UEs). Here, $R_i^f(t) = \beta R_i^f(t-1) + (1-\beta)\delta_i^f(t-1)r_{i,\text{actual}}^f(t-1)$, with $\beta = 0.99$ and $\delta_i^f(t-1)$ being the indicator that link i was scheduled for flow f in time slot $t-1$. Here, $r_{i,\text{actual}}^f(t-1)$ is the actual data rate of the scheduled flow f on link i at time $t-1$ (considering interference that resulted as an outcome of the scheduling decision in the previous time slot). Under the assumption of NNHR, scheduling is done using the computed priorities as follows. We pack in links with at least one non-zero priority flow in descending order of the highest priority flow through a link, respecting the half duplex constraint of the devices. If a link is scheduled as per this criterion, then the flows corresponding to highest priority on the scheduled links are chosen in that particular slot for scheduling. This is a greedy variant of the algorithm considered in [42] since

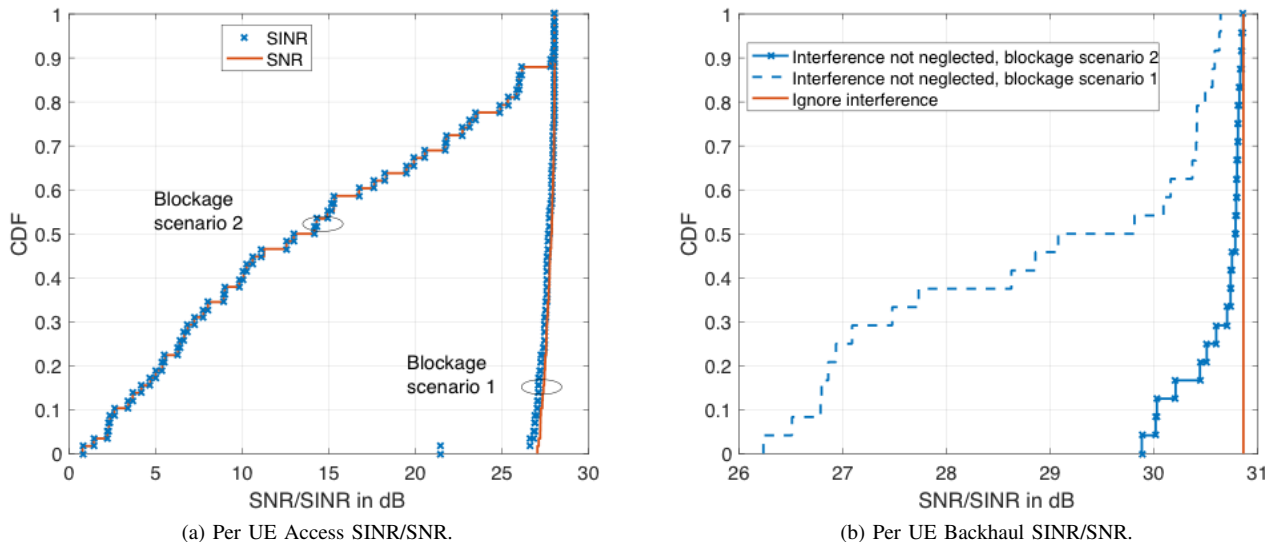


Fig. 8: SINR vs SNR considering the greedy PF scheduler.

instead of searching over all possible transmission schedules we pick a greedy schedule in descending order of priorities.

Fig. 7(b) shows the distribution of achieved per user e2e rates for the topology in Fig. 5(a), which is computed by dividing the total number of bits received by the UEs from the MBS during a simulation run of 10000 iterations with 0.2 ms slot duration. Data for SINR/SNR and e2e rate was collected after 1000 warm-up iterations and queues at the relays were empty initially. Two blockage scenarios were considered. Scenario 1 implies all links along the same street are LOS to create a worst case interference scenario. Scenario 2 implies only neighbouring backhaul links are LOS, and rest are NLOS. This is reasonable since the non-neighbouring BSs are at least 400m apart, which will likely lead to NLOS links [5], [37]. Scenario 2 also assumes that access links are all NLOS to generate a scenario with low access SNRs. Fig. 8 shows the access and backhaul SINR versus SNR comparison in the two blockage scenarios. It can be seen from Fig. 7(b) that the rate distribution is almost vertical, implying equal rate per UE was achieved. Ignoring interference, the rate is exactly equal to the max-min rate from our analysis (also equal to 137 Mbps as in Table II), which is surprising at first but can be explained as follows. The bottleneck links for all UEs are those connected to the fiber site having a constant rate R_1 . Thus, irrespective of whether we do PF or max-min fair scheduling the rates coincide¹. Note that there is a small drop in rates (by 10%) with interference when all interferers on the same street are LOS. In blockage scenario 2, it is found that the rates with interference do not change at all. This confirms the noise-limited behaviour of the network under consideration.

An intuitive observation that explains noise-limitedness for DL scenario is as follows. All backhaul links operate in a direction away from the fiber site. This along with NNHR

ensures that the bottleneck backhaul links connected to the fiber site never see interference with beams aligned towards their receivers from other backhaul links. Nearby access links pointing towards the ring 1 are also rarely activated since the ring 2 relays have to backhaul traffic for ring 3 relays. This leads to low interference on bottleneck links.

VII. CONCLUSIONS AND FUTURE WORK

A baseline model to study e2e rates in self-backhauled mmWave networks with multiple backhaul hops is presented. The model is used to derive maximum achievable rates by all UEs in the network as a function of number of relays per fiber site. Apart from the simplicity in the derived formulae, a key takeaway is that noise-limitedness in the k -ring deployment is aided by the observation that there are a few bottleneck links in the network making it sufficient for a max-min scheduler to activate only a few links at a time. We believe that to bridge the gap in theory and practise while studying the performance of multi-hop mmWave networks it is essential to considering network planning along with resource allocation in order to exploit the unique interactions of mmWave propagation with the deployment scenarios considered.

Studying the robustness of access and backhaul link-failures in multi-hop mmWave networks is a possible scope of future research. If a backhaul link fails, there are two possible options – re-route the traffic on an alternate path or use the NLOS backhaul link. If an access link fails, multi-connectivity with mmWave or sub-6GHz BSs can be explored to provide robustness to dynamic blockages. Another direction would be to understand latency performance considering the k -ring deployment model. It is likely that max-min or PF schedulers have poor delay performance, and thus newer optimization problems that offer different rates to relays on different rings may be required to bound the delay performance within the 1ms latency requirement for 5G.

¹Since UE rates on the fiber backhaul links add up to a constant, the solution of PF is same as max-min.

APPENDIX A
PROOF OF THEOREM 1.

Let γ be the minimum e2e rate that all UEs can achieve. Knowing the instantaneous rates of the links and the loads, let us now write down necessary conditions for γ to be minimum achievable e2e rate, assuming NNHR. The following inequality needs to hold considering the scheduling done by the MBS.

$$\gamma \left(\frac{w_{0,0}}{R_a} + \frac{f(0,0) - w_{0,0}}{R_1} \right) \leq 1. \quad (2)$$

Here, left hand side is the total time a BS is active (either transmitting or receiving) and right hand side is the total available time. Here, $\frac{\gamma}{R_a}$ is the minimum fraction of time utilized by MBS for serving a UE directly connected to it on access link. Since there are $w_{0,0}$ such UEs, $\frac{\gamma w_{0,0}}{R_a}$ is the minimum fraction of time MBS spends on access links. Similarly, $\frac{\gamma}{R_1}$ is the minimum fraction of time the MBS spends to serve any indirectly connected user by wireless backhauling. Since there are $f(0,0) - w_{0,0}$ such users, we have the required inequality.

Similarly, one can write down inequalities considering minimum fraction of time other BSs need to be active to allow γ as the minimum achievable rate to all UEs. Considering the BS at (i, j) , with at least i or j not equal to 0, the following inequality can be written.

$$\gamma \left(\frac{w_{i,j}}{R_a} + \frac{f(i,j) - w_{i,j}}{R_1} + \frac{f(i,j)}{R_1} \right) \leq 1,$$

where $\frac{f(i,j) - w_{i,j}}{R_1}$ is the minimum fraction of time the BS has to allocate for backhauling to relays connected to it, further away from $(0,0)$, and $\frac{f(i,j)}{R_1}$ is the minimum fraction of time the BS is served by its parent BS towards the MBS. Since $w_{i,j} = w_{-i,-j}$ and NNHR, we have $f(i,j) = f(-i,-j)$. Thus, the inequality can be written down as

$$\gamma \left(\frac{w_{i,j}}{R_a} + \frac{f(-i,-j) + f(i,j) - w_{i,j}}{R_1} \right) \leq 1. \quad (3)$$

Since $w_{0,0} > w_{i,j}$ and $f(i,j) + f(-i,-j) - w_{i,j} \leq f(i,j) + f(-i,-j) \leq f(0,0) - w_{0,0}$, the inequality (2) is stricter than (3). Thus, the bottleneck inequality is always (2) and thus, $\gamma \leq \left(\frac{w_{0,0}}{R_a} + \frac{f(0,0) - w_{0,0}}{R_1} \right)^{-1}$.

If we prove that a scheduler with NNHR helps achieve the above upper bound, then γ^* is the max-min rate. Consider the scheduler in Algorithm 1. If a UE is connected to the MBS, it is clear from the algorithm that its long term rate is γ^* since the user gets γ^*/R_a fraction of time with instantaneous rate R_a . If a UE is connected to the BS at (i', j') , then to ensure its long term rate is γ^* we need all the backhaul hops to support at least γ^* long term rate for the data of this particular user. Also we need the long term access rate for the UE to be at least γ^* . Since Algorithm 1 allocates $\gamma^* f(i, j)/R_1$ fraction of total time for serving a backhaul link with destination (i, j) and this time is equally divided amongst $f(i, j)$ UEs, the long term rate for any UE amongst the $f(i, j)$ UEs served on this link equals γ^* . Similarly, the fraction of time any user gets for access is at least γ^*/R_a , which implies long term rate of

γ^* . Thus, the upper bound γ^* is achievable and the max-min rate is given by γ^* if the routing is NNHR.

Consider any other routing strategy wherein the fiber site activates only nearest neighbour backhaul links. Note that inequality in (2) still needs to be satisfied as $f(0,0)$ is independent of the routing. Thus, if the nearest neighbour highway routes are changed such that the new links added to the routes do not directly connect with the MBS, it does not change the max-min rates. The only way γ^* is not global optimal is if a non-nearest neighbour backhaul links is activated by the fiber site and it outperforms NNHR. If possible, let the MBS serve some of the traffic on links that are not just limited to ring 1 relays. The new equal rate to all UEs, $\tilde{\gamma}$, has to satisfy the following inequality.

$$\tilde{\gamma} \left(\frac{w_{0,0}}{R_a} + \frac{\beta_1 (f(0,0) - w_{0,0})}{R_1} + \frac{\beta_2 (f(0,0) - w_{0,0})}{R_2} + \dots + \frac{\beta_k (f(0,0) - w_{0,0})}{R_k} \right) \leq 1,$$

where $\sum_{q=1}^k \beta_q = 1$ and $\beta_1 < 1$. Since $R_1 > R_2 > \dots > R_k$, we have that $\tilde{\gamma}$ will always be less than that obtained with NNR. Similarly, modifying any of the inequalities in (3) to serve some traffic on links with rates $< R_1$ leads to smaller max-min rates as compared to γ^* .

ACKNOWLEDGMENTS

The authors thank Gustavo de Veciana, Matthew Andrews, Eugene Visotsky, Mark Cudak for helpful discussions in the course of this work. The authors thank Manan Gupta for help with Fig. 2. The authors especially thank Gustavo de Veciana for help in identifying the optimization formulation in this work.

REFERENCES

- [1] Z. Pi and F. Khan, "An introduction to millimeter-wave mobile broadband systems," *IEEE Commun. Mag.*, vol. 49, no. 6, pp. 101–107, Jun. 2011.
- [2] "Making 5G NR a reality," Qualcomm, Tech. Rep., Dec. 2016. [Online]. Available: <https://bit.ly/2Fyhw>
- [3] S. Singh, M. N. Kulkarni, A. Ghosh, and J. G. Andrews, "Tractable model for rate in self-backhauled millimeter wave cellular networks," *IEEE J. Sel. Areas Commun.*, vol. 33, no. 10, pp. 2196–2211, Oct. 2015.
- [4] T. Rappaport *et al.*, "Millimeter wave mobile communications for 5G cellular: It will work!" *IEEE Access*, vol. 1, pp. 335–349, May 2013.
- [5] A. Karttunen *et al.*, "Spatially consistent street-by-street path loss model for 28-GHz channels in micro cell urban environments," *IEEE Trans. Wireless Commun.*, vol. 16, no. 11, pp. 7538–7550, Nov 2017.
- [6] T. Bai and R. W. Heath Jr., "Coverage and rate analysis for millimeter wave cellular networks," *IEEE Trans. Wireless Commun.*, vol. 14, no. 2, pp. 1100–1114, Oct. 2014.
- [7] J. G. Andrews *et al.*, "Modeling and analyzing millimeter wave cellular systems," *IEEE Trans. Commun.*, vol. 65, no. 1, pp. 403 – 430, Jan. 2017.
- [8] B. Hajek and G. Sasaki, "Link scheduling in polynomial time," *IEEE Trans. Inf. Theory*, vol. 34, no. 5, pp. 910–917, Sep 1988.
- [9] L. Tassiulas and A. Ephremides, "Stability properties of constrained queueing systems and scheduling policies for maximum throughput in multihop radio networks," *IEEE Trans. Autom. Control*, vol. 37, no. 12, pp. 1936–1948, Dec 1992.
- [10] F. P. Kelly, A. K. Maulloo, and D. K. H. Tan, "Rate control for communication networks: shadow prices, proportional fairness and stability," *J. Oper. Res. Soc.*, vol. 49, no. 3, pp. 237–252, Mar 1998.

- [11] K. Jain, J. Padhye, V. N. Padmanabhan, and L. Qiu, "Impact of interference on multi-hop wireless network performance," *Wireless Networks*, vol. 11, no. 4, pp. 471–487, Jul 2005.
- [12] P. Gupta and P. R. Kumar, "The capacity of wireless networks," *IEEE Trans. Inf. Theory*, vol. 46, no. 2, pp. 388–404, March 2000.
- [13] M. Franceschetti, O. Dousse, D. N. C. Tse, and P. Thiran, "Closing the gap in the capacity of wireless networks via percolation theory," *IEEE Trans. Inf. Theory*, vol. 53, no. 3, pp. 1009–1018, March 2007.
- [14] I. Gitman, "On the capacity of slotted ALOHA networks and some design problems," *IEEE Trans. Commun.*, vol. 23, no. 3, pp. 305–317, Mar 1975.
- [15] L. Kleinrock and J. Silvester, "Spatial reuse in multihop packet radio networks," *Proc. IEEE*, vol. 75, no. 1, pp. 156–167, Jan 1987.
- [16] M. Sikora, J. N. Laneman, M. Haenggi, D. J. Costello, and T. E. Fuja, "Bandwidth- and power-efficient routing in linear wireless networks," *IEEE Trans. Inf. Theory*, vol. 52, no. 6, pp. 2624–2633, June 2006.
- [17] "Part 11: Wireless LAN MAC and PHY specifications amendment 10: Mesh networking," *IEEE Std 802.11s*, Sept 2011.
- [18] 3GPP, "Evolved Universal Terrestrial Radio Access (E-UTRA); Relay radio transmission and reception; Release 11," TR 36.826, 2012.
- [19] S. W. Peters and R. W. Heath Jr., "The future of WiMAX: Multihop relaying with IEEE 802.16j," *IEEE Commun. Mag.*, vol. 47, no. 1, pp. 104–111, January 2009.
- [20] J. Andrews *et al.*, "Rethinking information theory for mobile ad hoc networks," *IEEE Commun. Mag.*, vol. 46, no. 12, pp. 94–101, Dec. 2008.
- [21] R. Mudumbai, S. K. Singh, and U. Madhow, "Medium access control for 60 GHz outdoor mesh networks with highly directional links," in *Proc. IEEE Infocom*, April 2009, pp. 2871–2875.
- [22] D. Yuan, H.-Y. Lin, J. Widmer, and M. Hollick, "Optimal joint routing and scheduling in millimeter-wave cellular networks," *Proc. IEEE INFOCOM*, 2018, to appear.
- [23] F. B. Tesema, A. Awada, I. Viering, M. Simsek, and G. P. Fettweis, "Mobility modeling and performance evaluation of multi-connectivity in 5G intra-frequency networks," in *Proc. IEEE Globecom Workshops*, Dec 2015, pp. 1–6.
- [24] J. García-Rois *et al.*, "On the analysis of scheduling in dynamic duplex multihop mmWave cellular systems," *IEEE Trans. Wireless Commun.*, vol. 14, no. 11, pp. 6028–6042, Nov. 2015.
- [25] M. N. Islam, S. Subramanian, and A. Sampath, "Integrated access backhaul in millimeter wave networks," in *Proc. IEEE Wireless Communications and Networking Conference (WCNC)*, 2017.
- [26] Z. He, S. Mao, S. Kompella, and A. Swami, "Minimum time length scheduling under blockage and interference in multi-hop mmWave networks," in *Proc. IEEE Globecom*, Dec 2015, pp. 1–7.
- [27] J. Du, E. Onaran, D. Chizhik, S. Venkatesan, and R. A. Valenzuela, "Gbps user rates using mmWave relayed backhaul with high gain antennas," *IEEE J. Sel. Areas Commun.*, vol. 35, no. 6, pp. 1363 – 1372, June 2017.
- [28] M. E. Rasekh, D. Guo, and U. Madhow, "Interference-aware routing and spectrum allocation for millimeter wave backhaul in urban picocells," in *Proc. Allerton*, Sept 2015, pp. 1–7.
- [29] Y. Li, J. Luo, W. Xu, N. Vucic, E. Pateromichelakis, and G. Caire, "A joint scheduling and resource allocation scheme for millimeter wave heterogeneous networks," in *Proc. IEEE WCNC*, March 2017, pp. 1–6.
- [30] M. N. Kulkarni, J. G. Andrews, and A. Ghosh, "Performance of dynamic and static TDD in self-backhauled millimeter wave cellular networks," *IEEE Trans. Wireless Commun.*, vol. 16, no. 10, pp. 6460–6478, Oct 2017.
- [31] E. Guttman, "5G new radio and system standardization in 3GPP," 3GPP TSG SA Chairman, Tech. Rep., March 2017. [Online]. Available: <https://bit.ly/2qM23Lx>
- [32] "The 5G mmWave revolution," Nokia, Tech. Rep., 2016, available at <https://goo.gl/6XBxks>.
- [33] Y. Wang, K. Venugopal, A. F. Molisch, and R. W. Heath Jr., "MmWave vehicle-to-infrastructure communication: Analysis of urban microcellular networks," *IEEE Trans. Veh. Technol.*, April 2018, to appear. Available at arXiv:1702.08122.
- [34] Z. Zhang, J. Ryu, S. Subramanian, and A. Sampath, "Coverage and channel characteristics of millimeter wave band using ray tracing," in *Proc. IEEE ICC*, June 2015, pp. 1380–1385.
- [35] M. O. Hasna and M. S. Alouini, "Outage probability of multihop transmission over Nakagami fading channels," *IEEE Commun. Lett.*, vol. 7, no. 5, pp. 216–218, May 2003.
- [36] M. N. Kulkarni, E. Visotsky, and J. G. Andrews, "Correction factor for analysis of MIMO wireless networks with highly directional beamforming," *IEEE Wireless Commun. Lett.*, 2018, to appear. Available at <https://arxiv.org/abs/1710.07369>.
- [37] M. R. Akdeniz *et al.*, "Millimeter wave channel modeling and cellular capacity evaluation," *IEEE J. Sel. Areas Commun.*, vol. 32, no. 6, pp. 1164–1179, June 2014.
- [38] Ericsson. (2017) Designing for the future: the 5G NR physical layer. Available at <https://goo.gl/jU5S1r>.
- [39] T. Dinc and H. Krishnaaswamy, "Millimeter-wave full-duplex wireless: Applications, antenna interfaces and systems," in *Proc. IEEE Custom Integrated Circuits Conference (CICC)*, April 2017, pp. 1–8.
- [40] P. Mogensen *et al.*, "LTE capacity compared to the Shannon bound," in *Proc. IEEE VTC Spring*, April 2007, pp. 1234–1238.
- [41] M. N. Kulkarni. (2018, March) MATLAB codes for multi-hop mmWave cellular networks. Available at: <https://goo.gl/VoAjWm>.
- [42] U. Akyol *et al.*, "Joint scheduling and congestion control in mobile ad-hoc networks," in *IEEE INFOCOM*, April 2008.